Identification and functional prediction of anthocyanin biosynthesis regulatory long non-coding RNAs (lncRNAs) in carrot

Constanza Chialva[1#], Thomas Blein[2#], Martin Crespi[2*] & Diego Lijavetzky[1*]

[1]Instituto de Biología Agrícola de Mendoza (IBAM), UNCuyo, CONICET, Facultad de Ciencias Agrarias, Almirante Brown 500, M5528AHB, Chacras de Coria, Mendoza, Argentina. [2]Institute of Plant Sciences Paris-Saclay (IPS2), CNRS, INRA, University Paris-Saclay and University of Paris Batiment 630, Gif Sur Yvette, France.

[#]Constanza Chialva and Thomas Blein contributed equally to this work.

[*]Correspondence and requests for materials should be addressed to D.L. (email: dlijavetzky@conicet.gov.ar) or M.C. (email: martin.crespi@ips2.universite-paris-saclay.fr)

ABSTRACT

Carrot (*Daucus carota* L.) is one of the most cultivated vegetable in the world and of great importance in the human diet. Its storage organs can accumulate large quantities of anthocyanins, metabolites that confer the purple pigmentation to carrot tissues and whose biosynthesis is well characterized. Long non-coding RNAs (lncRNAs) play critical roles in regulating gene expression of various biological processes in plants. In this study, we used a high throughput stranded RNA-seq to identify and analyze the expression profiles of lncRNAs in phloem and xylem root samples using two genotypes with a strong difference in anthocyanin production. We identified 639 differentially expressed lncRNAs between genotypes, and certain were specifically associated with a particular tissue. We then established regulatory correlations between lncRNAs and anthocyanin biosynthesis genes in order to identify a molecular framework for the differential expression of the pathway between genotypes. A specific natural antisense transcript (NAT) linked to the *DcMYB7* key anthocyanin biosynthetic transcription factor suggested how the regulation of this pathway may have evolved between genotypes.

INTRODUCTION

Anthocyanins are flavonoids, a class of phenolic compounds synthesized via the phenylpropanoid pathway, a late branch of the shikimic acid pathway[1]. They are secondary metabolites that confer purple, red, and blue pigmentation to several organs and tissues of many plant species[2]. These water-soluble pigments serve in various roles

in the plant, including attracting pollinators to flowers and seed dispersers to fruits, protection against UV radiation, amelioration of different abiotic and biotic stresses, such as drought, wounding, cold temperatures, and pathogen attacks[3,4], as well as participation in physiological processes such as leaf senescence[5,6]. As dietary components, anthocyanins possess various health-promoting effects, mainly due to their antioxidant and anti-inflammatory properties, including protection against cancer, strokes and other chronic human disorders[7].

Carrot (*Daucus carota* subsp. *carota* L.; 2n = 2x = 18) is a globally important root crop with yellow and purple as the first documented colors for domesticated carrot in Central Asia approximately 1,100 years ago[8]. Orange carrots were not reliably reported until the sixteenth century in Europe[9,10], where its popularity was fortuitous for modern consumers because the orange pigmentation results from high quantities of α- and β-carotene, making carrots the richest source of provitamin A in the US diet[11]. Additionally, with its great nutrition and economic value, carrot has been well known as a nice model plant for genetic and molecular studies[11]. Carrot is one of the crops that can accumulate large quantities of anthocyanins in its storage roots (up to 17–18 mg/100 g fresh weight)[12]. Purple carrots accumulate almost exclusively derivatives of cyanidin glycosides with five cyanidin pigments reported in most studies[13,14]. The root content of these five anthocyanin pigments vary across carrot genetic backgrounds[12,15]. In addition, anthocyanin pigmentation also varies between root tissues, ranging from fully pigmented roots (i.e., purple color in the root phloem and xylem) to pigmentation only in the outer-most layer of the phloem[16,17].

Regardless of the plant species, at least two classes of genes are involved in anthocyanin biosynthesis: structural genes encoding the enzymes that directly catalyze the production of anthocyanins, and regulatory genes that control the transcription of

structural genes[18,19]. In most cases, the anthocyanin biosynthetic structural genes are regulated by transcription factors (TFs) belonging to the R2R3–MYB, basic helix-loop-helix (bHLH) and WD-repeat protein families, in the form of the 'MBW' complex[19,20]. Recent reports pointed out that gene regulation by TFs may play a key role controlling anthocyanin pigmentation in purple carrots[17,21,22]. Moreover, the broad variation observed among purple carrot root genotypes, regarding both anthocyanin concentration and pigment distribution in the phloem and xylem tissues, suggests independent genetic regulation in these two root tissues[23]. In this sense, Xu et al.[16] found that the expression pattern of a R2R3–MYB TF, *DcMYB6*, is correlated with anthocyanins production in carrot roots and that the overexpression of this gene in *Arabidopsis thaliana* enhanced anthocyanins accumulation in vegetative and reproductive tissues in this heterologous system. Similarly, Kodama et al.[24] found that a total of 10 *MYB*, *bHLH* and *WD40* genes were consistently up- or downregulated in a purple color-specific manner, including *DcMYB6*. Iorizzo et al.[25] identified a cluster of MYB TFs, with *DcMYB7* as a candidate gene for root and petiole pigmentation, and *DcMYB11* as a candidate gene for petiole pigmentation. Bannoud et al.[23] showed that *DcMYB7* and *DcMYB6* participate in the regulation of phloem pigmentation in purple-rooted samples. Finally, Xu et al.[26], by means of lost- and gain-of-function mutation experiments, demonstrated that *DcMYB7* is the main determinant that controls purple pigmentation in carrot roots.

Non-coding RNAs with a length higher than 200 nucleotides are defined as long noncoding RNAs (lncRNAs). They were originally considered to be transcriptional byproducts, or transcriptional 'noise', and were often dismissed in transcriptome analyses due to their low expression and low sequence conservation compared with protein-coding mRNAs. However, specific lncRNAs were shown to be involved in chromatin modification, epigenetic regulation, genomic imprinting, transcriptional

control as well as pre- and post-translational mRNA processing in diverse biological processes in plants[27–30]. Certain lncRNAs can be precursors of small interfering RNA (siRNA) or microRNA (miRNAs), triggering the repression of protein-coding genes at the transcription level (transcriptional gene silencing or TGS) or at post-transcriptional level (PTGS)[27,31]. Additionally, other lncRNAs can act as endogenous target mimics of miRNAs, to fine-tune the miRNA-dependent regulation of target genes[32,33]. It has been suggested that lncRNAs can regulate gene expression in both the *cis*- and *trans*-acting mode[34]. The *cis*-acting lncRNAs can be classified by their relative position to annotated genes[27,35,36] and notably include long noncoding natural antisense (lncNATs) transcribed in opposite strand of a coding gene, overlapping with at least one of its exons[37,38]. Other so-called intronic lncRNAs are transcribed within introns of a protein-coding gene[39] whereas long intergenic ncRNAs (lincRNAs) are transcripts located farther than 1 kb from protein-coding genes[27,35,36]. Among these cis-lncRNAs, NATs are of special interest as they have been shown to provide a mechanism for locally regulating the transcription or translation of the target gene on the other strand, providing novel mechanisms involved in the regulation of key biological processes[40] and environmentally dependent gene expression[37,38].

As mentioned above, several differential expression analyses have been performed between purple and non-purple carrot roots allowing the identification of the main structural genes and TFs involved in anthocyanin biosynthesis in whole roots and/or phloem tissues[16,21,23–26]. However, the identification and functional prediction of lncRNA in carrot or putatively involved in carrot anthocyanin biosynthesis regulation has not yet been reported. In the present study, we combined a high throughput stranded RNA-Seq based approach with a dedicated bioinformatic pipeline, to annotate lncRNAs and analyze the expression profiles of lncNATs putatively associated to the carrot root

anthocyanin biosynthesis regulation. In addition, we individually analyzed the gene expression patterns in phloem and xylem root of purple and orange *D. carota* genotypes. Our findings point for a role of antisense transcription in the anthocyanin biosynthesis regulation in the carrot root at a tissue-specific level.

RESULTS

RNA-seq data mining, identification and annotation of anthocyanin-related lncRNAs

In order to thoroughly identify and annotate lncRNAs related to anthocyanin biosynthesis regulation in carrot roots, we performed a whole transcriptome RNA-seq analysis of the carrot genotypes 'Nightbird' (purple phloem and xylem) and 'Musica' (orange phloem and xylem) that had been studied in a tissue specific manner (Supplementary Figure S1). We generated an average of 51.4 million of reads per sample from the 12 carrot root samples (i.e., two phenotypes x two tissues x three biological replicates), ranging from 43.5 million to 60.3 million. The average GC content (%) was 44.8% and the average ratio of bases that have phred[41] quality score of over 30 (Q30) was 94.1%. The average mapping rate to the carrot genome was 90.9% (Supplementary Table S1). We identified and annotated 8484 new transcripts, including 2095 new protein-coding transcripts and 6373 noncoding transcripts (1521 lncNATs, 4852 lincRNAs and 16 structural transcripts) (Supplementary Table S2 and Supplementary File S1). Those were added to the 34263 known carrot transcripts[42] to conform the final set of 42747 transcripts used for this work. The set contains 34204 coding transcripts and 7288 noncoding transcripts (1521 lncNATs, 5767 lincRNAs) and

1255 structural transcripts (Fig 1A and Supplementary Table S3). Most noncoding transcripts presented less than 1000 bp long, being 400-800 bp the most frequent length class. Coding transcripts between 500-1000 bp long were the most frequent, while most structural transcripts presented less than 200 bp (Fig 1B). Noncoding transcripts predominantly presented one exon and unexpectedly[43], only one exon was also the most frequent class for coding transcripts (Fig 1C). Finally, we found no particular bias for the distribution of the noncoding transcripts along the nine carrot chromosomes (Fig 1D). As expected, the average expression level of the ncRNAs, measured in Transcripts Per Kilobase Million (TPMs), was lower than that of the mRNAs (Fig. 1E).

Variation in coding and noncoding expression was mainly explained by the anthocyanin-pigmentation phenotype difference between orange and purple carrots

We sampled orange and purple carrot genotypes in two different tissues, phloem and xylem (Supplementary Figure S1). Considering the global gene variation of the 12 evaluated libraries (i.e., three for each phenotype/tissue combination), the color phenotype was clearly the main source of variation (PC1, 49 %), while the tissue specificity factor was also important (PC2, 18%), but significantly lower than the root color phenotype effect (Fig. 2A).

We then assessed the variation in mRNA and ncRNA gene expression between purple and orange carrot roots in our RNA-seq analysis. A total of 3567 genes were differentially expressed (DEG) between purple and orange carrots (Bonferroni's adjusted p-value < 0.01), divided in 2928 mRNA and 639 lncRNAs (Fig. 2B) and representing 10% and 15% of the mRNA and lncRNA expressed genes, respectively. Within the 3567 DEGs, we found 1664 downregulated and 1907 upregulated

167 transcripts. In turn, the downregulated transcripts were distributed into 1343 coding and
168 319 noncoding transcripts, while the upregulated were divided into 1585 and 320
169 coding and noncoding transcripts, respectively (Fig. 2B). All information concerning
170 the differentially expressed analysis and gene annotation is detailed in Supplementary
171 Table S4.
172 As expected, we identify several differentially expressed genes (DEG) between the two
173 genotypes known to be involved in carrot root anthocyanin biosynthesis[21,23–26]. Most of
174 the known genes of the pathway and their main regulators were differentially expressed
175 between the two genotypes (Supplementary Table S4). Several genes were induced in
176 purple tissues and they mainly comprised genes representing: i) the early step in the
177 flavonoid/anthocyanin pathway, like chalcone synthase (*DcCHS1*/DCAR_030786);
178 chalcone isomerase (*DcCHI1*/DCAR_027694) and (*DcCHIL*/DCAR_019805);
179 flavanone 3-hydroxylase (*DcF3H1*/DCAR_009483), and flavonoid 3′-hydroxylase
180 (*DcF3'H1*/DCAR_014032); ii) cytochrome P450 (CYP450) proteins, putatively related
181 to the flavonoid and isoflavonoid biosynthesis pathways[23,44]; iii) ATP-binding cassette
182 (ABC) transporters, potentially related to anthocyanin transport[45,46]; and iv) genes from
183 the late steps of the pathway, like dihydro-flavonol 4-reductase
184 (*DcDFR1*/DCAR_021485), leucoanthocyanidin dioxygenase (*DcLDOX1*/
185 DCAR_006772), and UDP-glycosyltransferase (*DcUFGT*/DCAR_009823) and the
186 recently described *DcUCGXT1*/DCAR_021269 and *DcSAT1*/MSTRG.8365, which
187 were confirmed to be responsible for anthocyanins glycosylation and acylation,
188 respectively[26,47]. Finally, most significant regulatory genes of the pathway, belonging to
189 the MYB, bHLH and WD40 TF gene families[21,23–26] were also differentially expressed
190 between purple and orange genotypes (Supplementary Table S4). We further analyzed
191 the tissue differential expression distribution of those 26 'MBW' TFs and found that

192 *DcMYB6* and *DcMYB7*, the two most studied TFs associated with anthocyanin
193 biosynthesis regulation[23–26], were differentially expressed between purple and orange
194 carrots, both in phloem and xylem tissues (Supplementary Figure S2). Interestingly,
195 three genes recently described to be regulated by *DcMYB7*[26] (i.e. *DcbHLH3*,
196 *DcUCGXT1* and *DcSAT1*) also displayed no tissue specificity. *DcbHLH3* was described
197 as a co-regulator in anthocyanin biosynthesis, while *DcUCGXT1* and *DcSAT1*
198 participate in anthocyanin glycosylation and acylation, respectively[26,47]. Additionally,
199 seven TFs showed xylem preferential expression-specificity, while only one was
200 preferentially expressed specifically in phloem. Finally, differential expression of 11
201 TFs was just detected when the 12 libraries were jointly analyzed, presumably by
202 presenting significant but low expression differences (Supplementary Figure S2).
203
204 **Putative regulation of anthocyanin-related genes by carrot antisense lncRNAs**
205 In order to investigate the putative involvement of carrot lncRNAs in the regulation of
206 the anthocyanin biosynthesis in different carrot root tissues, we predicted the potential
207 targets of lncRNAs in *cis*-regulatory relationship, particularly those classified as natural
208 antisense transcripts (lncNATs). The selection of such lncRNAs was based in three
209 assumptions: i) both, the lncRNA and the putative target were differentially expressed
210 between purple and orange tissues (Supplementary Table S4); ii) the lncRNAs were
211 antisense of the target genes; and iii) the Pearson and Spearman correlation coefficients
212 between the expression levels of these genes were ≥ 0.70 or ≤ -0.70, and $p < 0.01$.
213 According to these criteria, we found 19 differentially expressed lncNATs, since the
214 lncRNAs were located in the antisense orientation (in the opposite strand) to a target
215 mRNA, being most of them fully overlapping pairs (Supplementary Table S4 and S5).
216 About 79% of those lncNATs were expressed in concordance with sense strand

transcript, while five out of the 19 presented discordant expression (i.e. when the lncNAT expression increase, the sense strand transcript was repressed) (Supplementary Table S4 and S5). Interestingly, we detected two lncNATs (MSTRG.27767/asDcMyb6 and MSTRG.9120/asDcMyb7) in antisense relationship to *DcMYB6* and *DcMYB7*, respectively, with concordant expression correlation (Fig. 3). *DcMYB6* showed a log2 fold-change of 7.6 with an adjusted *p*-value of $4.5\ 10^{-30}$, while *DcMYB7* presented a log2 fold-change of 11.7 with an adjusted *p*-value of $3.8\ 10^{-37}$. Accordingly, the two detected antisense lncRNAs also presented significant differential expression, where *asDcMYB6* displayed a log2 fold-change of 6.5 with an adjusted *p*-value of $2.1\ 10^{-13}$ and *asDcMYB7* presented a log2 fold-change of 6.1 with an adjusted *p*-value of $1.3\ 10^{-04}$ (Supplementary Table S4). Finally, the Pearson and Spearman correlation coefficients between the expression levels of each sense/antisense pair were ≥0.79 and *p*-value < 0.01 (Supplementary Table S5). On the other hand, as also detailed in Supplementary Table S4, two out of the four lncNATs showing discordant expression were found in the antisense relationship with disease resistance-like related genes (a predicted Catalase, and probable disease resistance protein At5g63020).

DISCUSION

The presence of color in flowers, fruits and other organs and tissues, plays several biological functions mostly driven by the adaptive behavior of plants in response to the environment[2,20,48,49]. But in turn, plant organ pigmentation have served as natural genetic markers since the early works of Mendel[50,51]. Anthocyanins are flavonoid pigments that accumulate in plant cell vacuoles[52] and are mainly responsible for most

tissue and organ coloration[19,20,48]. Genetic analyses using model plant species like Arabidopsis, petunia and maize allowed the identification of most structural genes in the anthocyanin biosynthesis pathway as well as the main regulatory genes controlling pigment synthesis. In carrot, anthocyanin pigmentation is responsible for the purple phenotype[9,53]. Two main genes, *P_1 and P_3*, have been identified in chromosome 3 and suggested to be responsible for the two independent mutations underlying the domestication of purple carrots[17]. Despite several carrot structural genes from the anthocyanin biosynthesis pathway have shown expression correlation with the purple phenotype[21,22], none of them co-localize with *P_1 and P_3*. Similar situation occurred in other plants like grapevine, where accumulation of anthocyanins correlated with the expression of several structural genes of the pathway but none of them co-localized with the 'color locus' in chromosome 2[54,55]. Finally, this discrepancy was solved by a study describing an insertion mutation in the promotor of a R2R3–MYB TF (i.e. *VviMybA1*)[56] explaining the lack of color of white grapevine cultivars. In the same direction, several recent works[16,23–25,47] focused on the role of carrot TFs putatively involved in the regulation of anthocyanin biosynthesis in purple genotypes, particularly those belonging to the 'MBW' complex (i.e., R2R3–MYB, basic helix-loop-helix -bHLH- and WD-repeat TFs). Two recent reports showed that three R2R3–MYB TFs are involved in the *P_1 and P_3* loci: *DcMYB113* has been suggested to correspond to *P_1*[47], while *DcMYB6* and *DcMYB7* were proposed as the two main candidate TFs underlying the carrot root anthocyanin pigmentation in the *P_3* locus[25]. However, knockdown and overexpression functional analyses demonstrated that *DcMYB7* (but not *DcMYB6*) is the *P_3* gene controlling purple pigmentation in carrot roots[26]. Likewise described for the grapevine *VviMybA1* gene[56], non-purple carrot genotypes seems to arise by an insertion mutation in the promoter region of *DcMYB7*[26], yet the authors imply the existence of an

267 additional genetic factor suppressing the expression of *DcMYB7* in non-purple
268 pigmented peridermal carrot root tissues.

269 In this work, we performed a thorough transcriptomic analysis by comparing two carrot
270 hybrids with contrasted anthocyanin pigmentation phenotypes (i.e. purple vs. orange),
271 both in phloem and xylem tissues. The study corroborates the involvement of the
272 principal reported structural genes of the anthocyanin biosynthesis pathway[21,22], but
273 mostly, the key TF genes reported as the main regulators explain the carrot purple
274 phenotype (i.e. *DcMYB6* and *DcMYB7*)[16,25,26]. Interestingly, the performed dissection
275 between phloem and xylem purple samples, allowed us to show that there is no tissue-
276 specific expression of such key genes, contrary to previously suggested for *DcMYB6*
277 and *DcMYB7*[16,23,25].

278 We showed here the first whole genome identification and annotation of lncRNAs in
279 carrot by combining a high throughput stranded RNA-Seq based approach with a
280 focused bioinformatic pipeline. Through this process, we identified 6373 novel
281 lncRNAs, as compared to the 915 sequences annotated in the original carrot genome
282 assembly[42]. Moreover, 10% of them (641 genes) can be defined as anthocyanin
283 biosynthesis-related lncRNAs since we found them differentially expressed between
284 purple and orange carrots. For the functional annotation of such lncRNAs, we focused
285 on those showing an antisense relationship to differentially expressed protein coding
286 genes, known (or putatively) involved in carrot anthocyanin biosynthesis and depicted
287 in the precedent paragraph. Additionally, the selected lncNATs had to present a
288 statistically significant Pearson and Spearman correlation with their putative targets.
289 This led us to identify 19 differentially expressed lncNATs between purple and orange
290 carrots. Interestingly, we found two of these lncNATs (*asDcMYB6* and *asDcMYB7*)
291 transcribed in opposite direction to *DcMYB6* and *DcMYB7*, respectively. Moreover,

292 *asDcMYB6* and *asDcMYB7* exhibited concordant expression patterns with their
293 corresponding sense transcripts opening the possibility that non-coding RNA antisense
294 transcription is a new player in the regulation of carrot anthocyanin biosynthesis,
295 putatively affecting the expression of *DcMYB7* (and/or *DcMYB6*). This regulation
296 maybe linked to the previously described genetic factors[26].
297 Antisense transcripts, particularly lncNATs, present in many genomes of diverse
298 kingdoms, showed either positively or negatively correlated expression with their
299 corresponding sense transcripts. In many cases, lncNATs regulate the expression of
300 their sense transcripts in a negative or positive way, by means of different
301 transcriptional or post-transcriptional mechanisms. In particular cases, upregulation of
302 sense gene expression may be explained by the participation of a lncNAT in the
303 inhibition of other factors at translational level, such as efficient translation initiation or
304 elongation[57–59].
305 In plants, both repression and activation roles have been assigned to some lncNATs in
306 response to environmental conditions. While *COOLAIR* and *COLDAIR* negatively
307 regulates *FLC* in vernalization responses[39,60], and *SVALKA* controls *CBF1* expression to
308 consequently regulate freezing tolerance[38], the expression of another member of the
309 *FLC* family (*MAF4*) is activated by the lncNAT MAS to fine-tune flowering time[37].
310 Anthocyanins are known to participate in abiotic stress responses and adaptation to
311 environmental variations[3,4,61], so the evolutionary role of the newly identified antisense
312 transcrpts *asDcMYB7* and *asDcMYB6* may be linked to the activation of anthocyanin
313 biosynthesis through *DcMYB7* and *DcMYB6*. Hence, our work hints to new antisense
314 regulations potentially involved in the variable expression of anthocyanin genes among
315 carrot ecotypes.
316

METHODS

Sample preparation and plant material

Total RNA was obtained independently from three biological replicates of phloem and xylem root samples of two *Daucus carota* L genotypes: 'Nightbird', a purple root hybrid (purple phloem and xylem) and 'Musica', a non-anthocyanin pigmentated root hybrid. Plants were germinated from seeds and roots were collected after 12 weeks. Frozen samples were grinded using liquid nitrogen and RNA was extracted using TRI Reagent® (Sigma-Aldrich) and purified using SV Total RNA Isolation System (Promega). RNA samples were quantified, and purity measured using a spectrophotometer (AmpliQuant AQ-07). RNA integrity and potential genomic DNA contaminations were checked through agarose gel electrophoresis.

Libraries construction and RNA sequencing

Twelve samples (two genotypes x two tissues x three biological replicates) were sent to the Macrogen sequencing service (Seoul, Korea). Once in destiny they were checked for total RNA integrity using a Bioanalyzer RNA Nano 6000 chip. All the samples qualified to proceed with the library construction having an RNA Integrity Number (RIN) ≥7. NGS transcriptomic libraries were constructed using a TruSeq Stranded mRNA LT Sample Prep Kit (Illumina). To verify the size of PCR enriched fragments, the template size distribution was checked on an Agilent Technologies 2100 Bioanalyzer using a DNA 1000 chip. The sequencing of libraries was performed as paired-end 101 bp reads on an Illumina HiSeq 2500 platform. The quality of the raw reads in the FastQ files was checked through FastQC[62] and were then trimmed for

sequencing adaptor and low quality sequences using Trimmomatic[63] using 'ILLUMINACLIP:TruSeq3-PE.fa:2:30:10 LEADING:21 TRAILING:21 MINLEN:30' as parameters. For removing reads corresponding to remaining ribosomal RNA, trimmed reads were mapped to the rRNA reference using SortMeRNA[64] using '--ref silva-bac-16s-id90.fasta --ref silva-bac-23s-id98.fasta --ref silva-euk-18s-id95.fasta --ref silva-euk-28s-id98.fasta --paired_in --fastx --log -e 1e-07 -a 4 -v' as parameters.

New transcripts assembling and lncRNA identification

Clean filtered reads were aligned on the *Daucus carota* genome[42] using the STAR aligner[65] using '--alignIntronMin 20 --alignIntronMax 20000 --outSAMtype BAM SortedByCoordinate --outReadsUnmapped Fastx' as parameters. Subsequently, the aligned reads were assembled by means of StringTie[66] and new transcripts were extracted and annotated using the GffCompare[67] program (GffCompare classes "u", "x", to adjust). Only new transcripts whose length was greater than 200nt were kept. The classification of the newly predicted transcript was performed according the following steps: i) the transcripts were classified as coding if their predicted open reading frame (ORF) was greater than 120 aa or if they were predicted as coding by CPC2[68] calculator and classify as structural RNA in case of homology with structural RNA (tRNA, rRNA, snRNA or snoRNA) or as non-coding in case of homology with known structured non-coding RNA (miRNA precursors, lncRNA). The transcript without any homology in Rfam and classified as non-coding par CPC2 were classified as non-coding.

Differential expression analysis

We performed a strand-specific read counting of coding and non-coding gene using on the carrot official annotation and the newly predicted genes of this study for each of the

12 aligned BAM files by means of the featureCount[70] software included in the Rsubread package[71]. The resulted count data was used for differential expression analysis with DEseq2[72]. Differentially expressed genes were declared as having a Bonferroni's adjusted *p*-value < 0.01. Reads corresponding to the strand specific expression of mRNAs and their lncNATs were visualized with the Integrative Genomics Viewer (IGV) software[73]. Additional Venn diagrams were performed with Venny v2.1[74].

REFERENCES

1. Herrmann, K. M. & Weaver, L. M. The Shikimate Pathway. *Annu. Rev. Plant Physiol. Plant Mol. Biol.* **50**, 473–503 (1999).
2. Harborne, J. B. & Williams, C. A. Advances in flavonoid research since 1992. *Phytochemistry* **55**, 481–504 (2000).
3. Koes, R. E., Quattrocchio, F. & Mol, J. N. M. M. The flavonoid biosynthetic pathway in plants: Function and evolution. *BioEssays* **16**, 123–132 (1994).
4. Shirley, B. W. Flavonoid biosynthesis: 'new' functions for an 'old' pathway. *Trends Plant Sci.* **1**, 377–382 (1996).
5. Hatier, J.-H. B. & Gould, K. S. Anthocyanin Function in Vegetative Organs. in *Anthocyanins* 1–19 (Springer New York, 2008). doi:10.1007/978-0-387-77335-3_1
6. Gould, K. S. & Lister, C. Flavonoid function in plants. *Flavonoids Chem. Biochem. Appl.* 397–441 (2006).
7. Lila, M. A. Anthocyanins and human health: An in vitro investigative approach. *Journal of Biomedicine and Biotechnology* **2004**, 306–313 (2004).

8. Iorizzo, M. *et al.* Genetic structure and domestication of carrot (Daucus carota subsp. sativus) (Apiaceae). *Am. J. Bot.* **100**, 930–938 (2013).

9. Simon, P. W. Domestication, Historical Development, and Modern Breeding of Carrot. in *Plant Breeding Reviews* 157–190 (John Wiley & Sons, Inc., 2010). doi:10.1002/9780470650172.ch5

10. Arscott, S. A. & Tanumihardjo, S. A. Carrots of Many Colors Provide Basic Nutrition and Bioavailable Phytochemicals Acting as a Functional Food. *Compr. Rev. Food Sci. Food Saf.* **9**, 223–239 (2010).

11. Simon, P. W., Pollak, L. M., Clevidence, B. A., Holden, J. M. & Haytowitz, D. B. Plant Breeding for Human Nutritional Quality. in *Plant Breeding Reviews* **31**, 325–392 (John Wiley & Sons, Inc., 2009).

12. Montilla, E. C., Arzaba, M. R., Hillebrand, S. & Winterhalter, P. Anthocyanin composition of black carrot (Daucus carota ssp. sativus var. atrorubens Alef.) Cultivars antonina, beta sweet, deep purple, and purple haze. *J. Agric. Food Chem.* **59**, 3385–3390 (2011).

13. Kammerer, D., Carle, R. & Schieber, A. Quantification of anthocyanins in black carrot extracts (Daucus carota ssp. sativus var. atrorubens Alef.) and evaluation of their color properties. *Eur. Food Res. Technol.* **219**, 479–486 (2004).

14. Kammerer, D., Carle, R. & Schieber, A. Detection of peonidin and pelargonidin glycosides in black carrots (Daucus carota ssp.sativus var.atrorubens Alef.) by high-performance liquid chromatography/electrospray ionization mass spectrometry. *Rapid Commun. Mass Spectrom.* **17**, 2407–2412 (2003).

15. Mazza, G. & Miniati, E. (Enrico). *Anthocyanins in fruits, vegetables, and grains*. (CRC Press, 1993).

16. Xu, Z. S., Feng, K., Que, F., Wang, F. & Xiong, A. S. A MYB transcription

417 factor, DcMYB6, is involved in regulating anthocyanin biosynthesis in purple
418 carrot taproots. *Sci. Rep.* **7**, 1–9 (2017).
419 17. Cavagnaro, P. F. *et al.* A gene-derived SNP-based high resolution linkage map of
420 carrot including the location of QTL conditioning root and leaf anthocyanin
421 pigmentation. *BMC Genomics* **15**, 1118 (2014).
422 18. Jaakola, L. *et al.* Expression of genes involved in anthocyanin biosynthesis in
423 relation to anthocyanin, proanthocyanidin, and flavonol levels during bilberry
424 fruit development. *Plant Physiol* **130**, 729–39 (2002).
425 19. Koes, R., Verweij, W. & Quattrocchio, F. Flavonoids: a colorful model for the
426 regulation and evolution of biochemical pathways. *Trends Plant Sci* **10**, 236–242
427 (2005).
428 20. Winkel-Shirley, B. Flavonoid biosynthesis. A colorful model for genetics,
429 biochemistry, cell biology, and biotechnology. *Plant Physiol* **126**, 485–493
430 (2001).
431 21. Yildiz, M. *et al.* Expression and mapping of anthocyanin biosynthesis genes in
432 carrot. *Theor. Appl. Genet.* **126**, 1–14 (2013).
433 22. Xu, Z. S. *et al.* Transcript profiling of structural genes involved in cyanidin-based
434 anthocyanin biosynthesis between purple and non-purple carrot (Daucus carota
435 L.) cultivars reveals distinct patterns. *BMC Plant Biol.* **14**, (2014).
436 23. Bannoud, F. *et al.* Dissecting the genetic control of root and leaf tissue-specific
437 anthocyanin pigmentation in carrot (Daucus carota L.). *Theor. Appl. Genet.* **132**,
438 2485–2507 (2019).
439 24. Kodama, M. *et al.* Identification of transcription factor genes involved in
440 anthocyanin biosynthesis in carrot (Daucus carota L.) using RNA-Seq. *BMC*
441 *Genomics* **19**, 811 (2018).

442 25. Iorizzo, M. *et al.* A Cluster of MYB Transcription Factors Regulates
443 Anthocyanin Biosynthesis in Carrot (Daucus carota L.) Root and Petiole. *Front.*
444 *Plant Sci.* **9**, 1927 (2018).
445 26. Xu, Z.-S., Yang, Q.-Q., Feng, K. & Xiong, A.-S. Changing Carrot Color:
446 Insertions in DcMYB7 Alter the Regulation of Anthocyanin Biosynthesis and
447 Modification. *Plant Physiol.* pp.00523.2019 (2019). doi:10.1104/pp.19.00523
448 27. Ariel, F., Romero-Barrios, N., Jégu, T., Benhamed, M. & Crespi, M. Battles and
449 hijacks: noncoding transcription in plants. *Trends Plant Sci.* **20**, 362–371 (2015).
450 28. Forestan, C. *et al.* Stress-induced and epigenetic-mediated maize transcriptome
451 regulation study by means of transcriptome reannotation and differential
452 expression analysis. *Sci. Rep.* **6**, 1–20 (2016).
453 29. Forestan, C. *et al.* Epigenetic signatures of stress adaptation and flowering
454 regulation in response to extended drought and recovery in Zea mays. *Plant Cell*
455 *Environ.* **43**, 55–75 (2020).
456 30. Mercer, T. R. & Mattick, J. S. Structure and function of long noncoding RNAs in
457 epigenetic regulation. *Nature Structural and Molecular Biology* **20**, 300–307
458 (2013).
459 31. Wu, H. J., Wang, Z. M., Wang, M. & Wang, X. J. Widespread long noncoding
460 RNAs as endogenous target mimics for microRNAs in plants. *Plant Physiol.* **161**,
461 1875–1884 (2013).
462 32. Zhang, G. *et al.* Transcriptomic and functional analyses unveil the role of long
463 non-coding RNAs in anthocyanin biosynthesis during sea buckthorn fruit
464 ripening. *DNA Res.* **25**, 465–476 (2018).
465 33. Yang, T. *et al.* Systematic identification of long noncoding <scp>RNA</scp> s
466 expressed during light-induced anthocyanin accumulation in apple fruit. *Plant J.*

100, 572–590 (2019).

34. Li, Z. & Rana, T. M. Molecular mechanisms of RNA-triggered gene silencing machineries. *Acc. Chem. Res.* **45**, 1122–1131 (2012).

35. Rinn, J. L. & Chang, H. Y. Genome Regulation by Long Noncoding RNAs. *Annu. Rev. Biochem.* **81**, 145–166 (2012).

36. Bonasio, R. & Shiekhattar, R. Regulation of Transcription by Long Noncoding RNAs. *Annu. Rev. Genet.* **48**, 433–455 (2014).

37. Zhao, X. *et al.* Global identification of Arabidopsis lncRNAs reveals the regulation of MAF4 by a natural antisense RNA. *Nat. Commun.* **9**, 1–12 (2018).

38. Kindgren, P., Ard, R., Ivanov, M. & Marquardt, S. Transcriptional read-through of the long non-coding RNA SVALKA governs plant cold acclimation. *Nat. Commun.* **9**, (2018).

39. Heo, J. B. & Sung, S. Vernalization-mediated epigenetic silencing by a long intronic noncoding RNA. *Science (80-.).* **331**, 76–79 (2011).

40. Thieffry, A. *et al.* Characterization of Arabidopsis thaliana promoter Bidirectionality and Antisense RNAs by Depletion of Nuclear RNA Decay Pathways. *Plant Cell* tpc.00815.2019 (2020). doi:10.1105/tpc.19.00815

41. Ewing, B., Hillier, L. D., Wendl, M. C. & Green, P. Base-calling of automated sequencer traces using phred. I. Accuracy assessment. *Genome Res.* **8**, 175–185 (1998).

42. Iorizzo, M. *et al.* A high-quality carrot genome assembly provides new insights into carotenoid accumulation and asterid genome evolution. *Nat. Genet.* **48**, 657–666 (2016).

43. Ramírez-Sánchez, O., Pérez-Rodríguez, P., Delaye, L. & Tiessen, A. Plant Proteins Are Smaller Because They Are Encoded by Fewer Exons than Animal

Proteins. *Genomics, Proteomics Bioinforma.* **14**, 357–370 (2016).

44. Ayabe, S. I. & Akashi, T. Cytochrome P450s in flavonoid metabolism. *Phytochemistry Reviews* **5**, 271–282 (2006).

45. Kovinich, N. *et al.* Arabidopsis MATE45 antagonizes local abscisic acid signaling to mediate development and abiotic stress responses. *Plant Direct* **2**, e00087 (2018).

46. Francisco, R. M. *et al.* ABCC1, an ATP Binding Cassette Protein from Grape Berry, Transports Anthocyanidin 3-O-Glucosides. *Plant Cell Online* (2013). doi:10.1105/tpc.112.102152

47. Xu, Z., Yang, Q., Feng, K., Yu, X. & Xiong, A. DcMYB113, a root-specific R2R3-MYB, conditions anthocyanin biosynthesis and modification in carrot. *Plant Biotechnol. J.* pbi.13325 (2020). doi:10.1111/pbi.13325

48. Mol, J., Grotewold, E. & Koes, R. How genes paint flowers and seeds. *Trends Plant Sci* **3**, 212–217 (1998).

49. Winkel-Shirley, B. Biosynthesis of flavonoids and effects of stress. *Curr Opin Plant Biol* **5**, 218–223 (2002).

50. Henig, R. M. *The monk in the garden: the lost and found genius of Gregor Mendel, the father of genetics*. (Houghton Mifflin Harcourt, 2017).

51. Hartl, D. L. & Orel, V. What did Gregor Mendel think he discovered? *Genetics* **131**, 245 (1992).

52. Petrussa, E. *et al.* Plant Flavonoids—Biosynthesis, Transport and Involvement in Stress Responses. *Int. J. Mol. Sci.* **14**, 14950–14973 (2013).

53. Simon, P. W. Inheritance and expression of purple and yellow storage root color in carrot. *J. Hered.* **87**, 63–66 (1996).

54. Kobayashi, S., Ishimaru, M., Ding, C. K., Yakushiji, H. & Goto, N. Comparison

of UDP-glucose:flavonoid 3-O-glucosyltransferase (UFGT) gene sequences between white grapes (Vitis vinifera) and their sports with red skin. *Plant Sci* **160**, 543–550 (2001).

55. Kobayashi, S., Ishimaru, M., Hiraoka, K. & Honda, C. Myb-related genes of the Kyoho grape (Vitis labruscana) regulate anthocyanin biosynthesis. *Planta* **215**, 924–933 (2002).

56. Kobayashi, S., Goto-Yamamoto, N. & Hirochika, H. Retrotransposon-induced mutations in grape skin color. *Science (80-.).* **304**, 982 (2004).

57. Pelechano, V. & Steinmetz, L. M. Gene regulation by antisense transcription. *Nature Reviews Genetics* **14**, 880–893 (2013).

58. Wight, M. & Werner, A. The functions of natural antisense transcripts. *Essays Biochem.* **54**, 91–101 (2013).

59. Faghihi, M. A. & Wahlestedt, C. Regulatory roles of natural antisense transcripts. *Nature Reviews Molecular Cell Biology* **10**, 637–643 (2009).

60. Swiezewski, S., Liu, F., Magusin, A. & Dean, C. Cold-induced silencing by long antisense transcripts of an Arabidopsis Polycomb target. *Nature* **462**, 799–802 (2009).

61. Rienth, M. *et al.* Day and night heat stress trigger different transcriptomic responses in green and ripening grapevine (vitis vinifera) fruit. *BMC Plant Biol.* **14**, 108 (2014).

62. Andrews, S. FastQC: a quality control tool for high throughput sequence data. (2010). Available at: https://www.bioinformatics.babraham.ac.uk/projects/fastqc/.

63. Bolger, A. M., Lohse, M. & Usadel, B. Trimmomatic: a flexible trimmer for Illumina sequence data. *Bioinformatics* **30**, 2114–2120 (2014).

64. Kopylova, E., Noé, L. & Touzet, H. SortMeRNA: fast and accurate filtering of ribosomal RNAs in metatranscriptomic data. *Bioinformatics* **28**, 3211–3217 (2012).

65. Dobin, A. *et al.* STAR: ultrafast universal RNA-seq aligner. *Bioinformatics* **29**, 15–21 (2013).

66. Pertea, M. *et al.* StringTie enables improved reconstruction of a transcriptome from RNA-seq reads. *Nat. Biotechnol.* **33**, 290–295 (2015).

67. GffCompare. A Program for processing GTF/GFF files. Available at: https://ccb.jhu.edu/software/stringtie/gffcompare.shtml.

68. Kang, Y.-J. *et al.* CPC2: a fast and accurate coding potential calculator based on sequence intrinsic features. *Nucleic Acids Res.* **45**, W12–W16 (2017).

69. Nawrocki, E. P. & Eddy, S. R. Infernal 1.1: 100-fold faster RNA homology searches. *Bioinformatics* **29**, 2933–2935 (2013).

70. Liao, Y., Smyth, G. K. & Shi, W. featureCounts: an efficient general purpose program for assigning sequence reads to genomic features. *Bioinformatics* **30**, 923–930 (2014).

71. Liao, Y., Smyth, G. K. & Shi, W. The R package Rsubread is easier, faster, cheaper and better for alignment and quantification of RNA sequencing reads. *Nucleic Acids Res.* **47**, e47–e47 (2019).

72. Love, M. I., Huber, W. & Anders, S. Moderated estimation of fold change and dispersion for RNA-seq data with DESeq2. *Genome Biol.* **15**, 550 (2014).

73. Thorvaldsdóttir, H., Robinson, J. T. & Mesirov, J. P. Integrative Genomics Viewer (IGV): high-performance genomics data visualization and exploration. *Brief. Bioinform.* **14**, 178–192 (2012).

74. Oliveros, J. C. Venny. *Venny. An interactive tool for comparing lists with Venn's*

diagrams. (2015).

ACKNOWLEDGEMENTS

This work was supported by Agencia Nacional de Promoción Científica y Tecnológica (ANPCyT): PICT2015-0822 & PICT-2016-3134; LabEx Sciences des Plantes de Saclay (SPS). Travel suport to Diego Lijavetzky was funded by Programa de Movilidad para Docentes de la UNCuyo, INRA and Universite Paris Sud. We thank to Dr. Pablo Cavagnaro for providing and growing the plant materials.

AUTHOR CONTRIBUTIONS

C.C. performed the samples collection, laboratory work for library preparation, participated in the draft of the manuscript and figures preparation; T.B. designed the bioinformatic pipeline related to raw data processing, new transcripts identification and differential expression analysis. M.C provided the main insight on the design of the transcriptomic experiment. D.L. wrote the final manuscript, designed and coordinated the experiments. All authors carefully read and helped to improve the final content of the manuscript.

ADDITIONAL INFORMATION

Data access: Sequence files generated during this study have been deposited into the NCBI BioProject database accession PRJNA668894.

Competing Interests: The authors declare no competing interests.

FIGURE LEGENDS

593 **Figure 1**. Characteristics of carrot transcripts. (A) Distribution of coding, noncoding
594 and structural sequences between the known and newly annotated transcripts. (B)
595 Transcript length distributions for the total coding, noncoding and structural RNAs. (C)
596 Number of exons per transcript for the total coding and noncoding RNAs. (D)
597 Proportional distribution of the total coding, noncoding and structural RNAs along each
598 chromosome. (E) Violin plot of the expression levels of carrot total coding and
599 noncoding RNAs. The y-axis represents the average log2(TPM) values. T-test *p*-value <
600 0.01 is considered to be significantly different.

601

602 **Figure 2**. Expression of carrot coding and noncoding RNAs. (A) PCA analysis of the
603 global gene expression of the 12 evaluated libraries (three replicates for each color-
604 phenotype and tissue type combination). (B) Differentially expressed genes (up- and
605 down-regulated) between purple and orange carrots (Bonferroni's adjusted *p*-value <
606 0.01) distributed by coding and noncoding transcripts.

607

608 **Figure 3**. Strand specific expression of R2R3–MYB TFs and their lncNATs. Coverage
609 data for the sense (green) and antisense (red) strands corresponding to
610 *DcMYB7*/*asDcMYB7* (A) and *DcMYB6/as DcMYB6* (B), respectively. Tracks
611 correspond to four carrot libraries: two phloem samples Purple_F1 and Orange F1; and
612 two xylem samples Purple_X1 and Orange_X1. Data Range of each track was set to
613 allow an even visualization of the mRNA and lncRNA transcripts by enlarging the last
614 ones (20x).

615

Supplementary Figure S1. Picture of the purple and orange hybrids used for the RNA-seq experiment and scheme of the performed dissection between xylem and phloem tissues.

Supplementary Figure S2. Tissue specific differential expression of the 26 'MBW' TFs identified in the experiment. a) Genes differentially expressed between purple and orange carrots both in xylem and phloem tissues; b) genes differentially expressed between purple and orange carrots just in xylem; c) gene differentially expressed between purple and orange carrots just in phloem; d) genes differentially expressed between purple and orange carrots detected after the join analysis of phloem and xylem samples.

Supplementary Table S1. Summary of NGS and quality control data regarding the 12 sequenced libraries.

Supplementary Table S2. Genome annotation of the newly identified transcripts.

Supplementary Table S3. Known and newly annotated carrot genes classified as coding, noncoding and structural transcripts.

Supplementary Table S4. Overall differentially expressed genes (DEGs) list, including statistical tests, *cis*-located sequences, gene lengths and gene products. The 21 identified lncNAT/coding transcript pairs are sorted on top of the list.

Supplementary Table S5. Pearson and Spearman correlation coefficients between the expression levels of the 19 identified lncNAT/coding transcript pairs across the 12 analyzed libraries.

Supplementary File S1. FASTA sequences of the newly annotated transcripts.

639

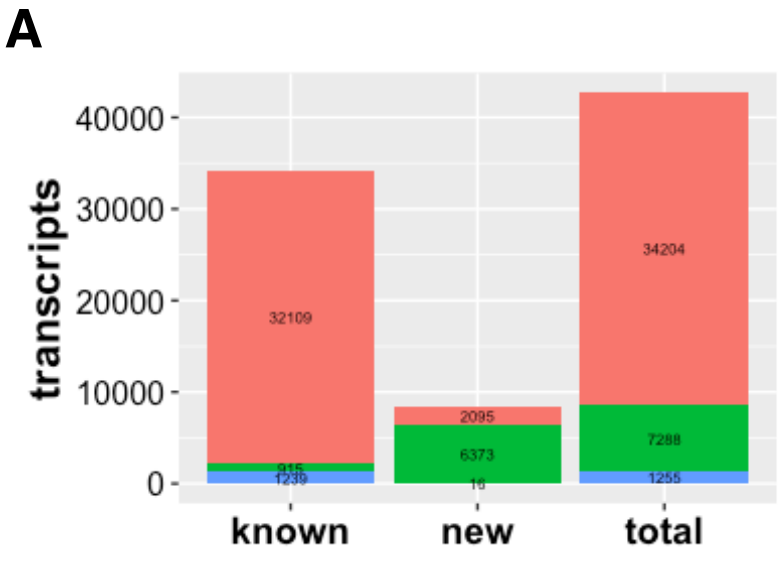

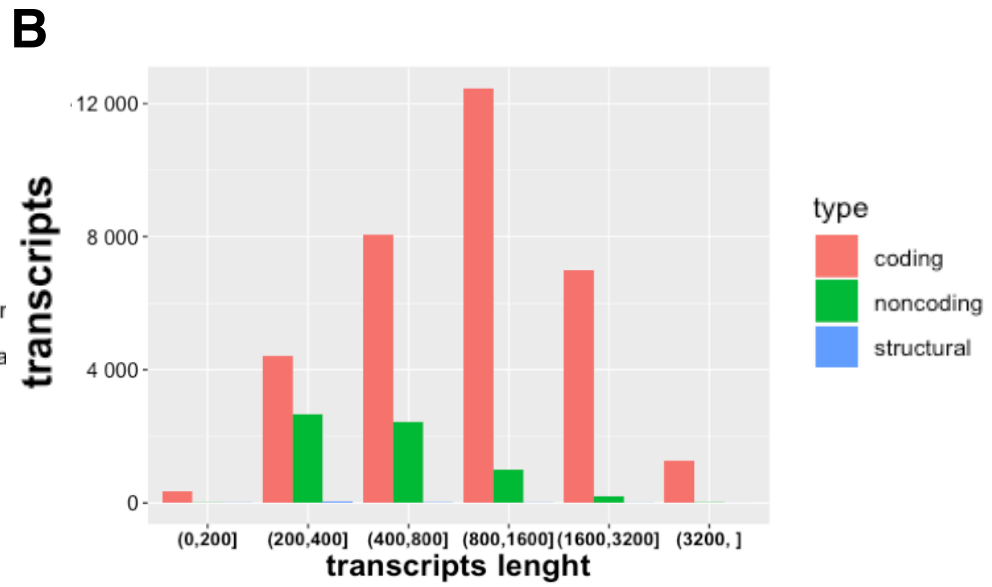

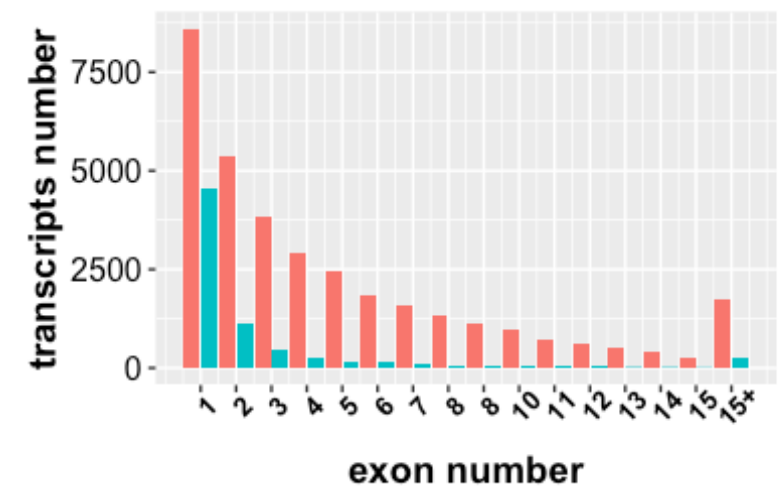

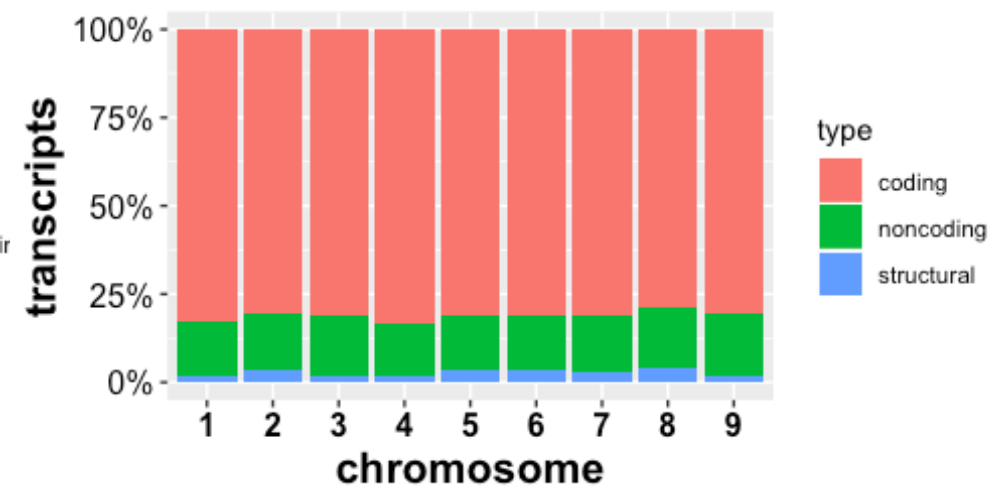

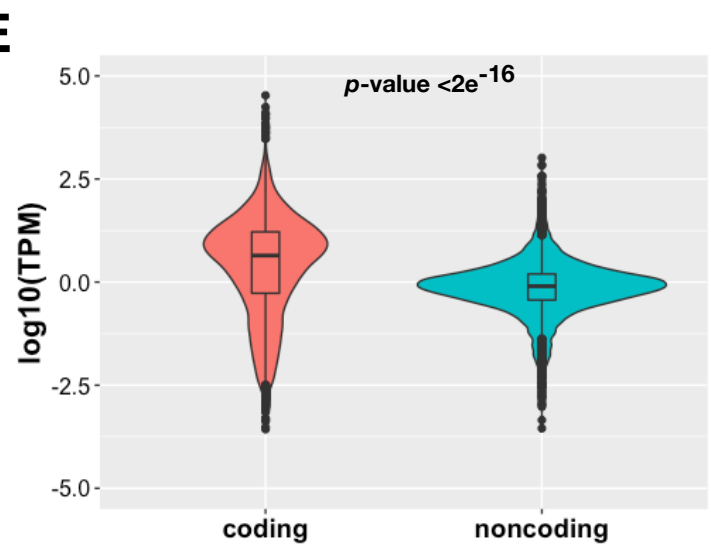

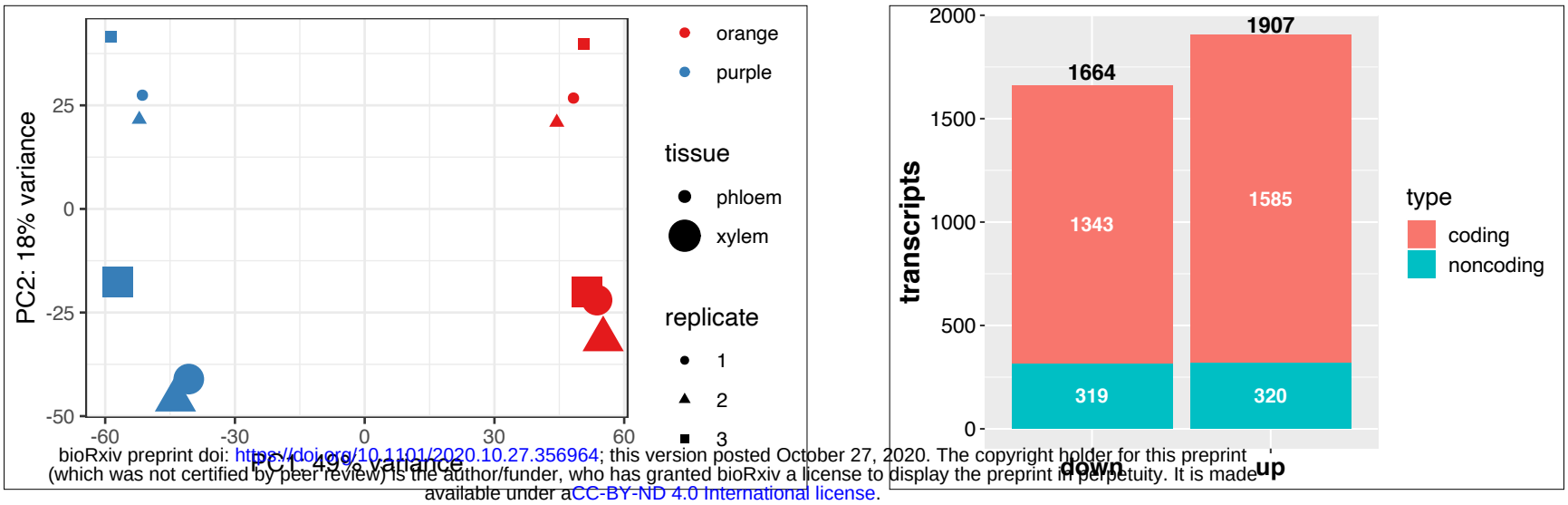

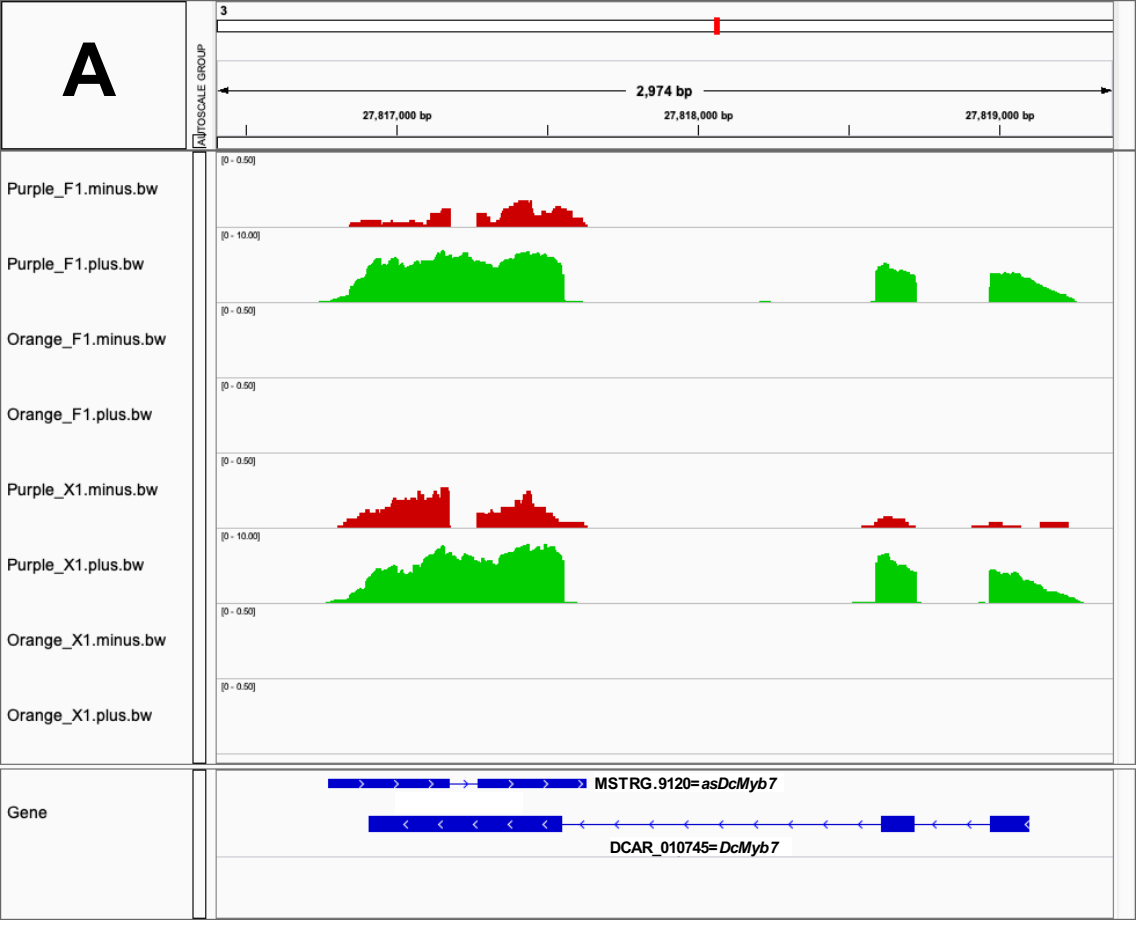
A
3
AUTOSCALE GROUP
2,974 bp
27,817,000 bp
27,818,000 bp
27,819,000 bp
Purple_F1.minus.bw
Purple_F1.plus.bw
Orange_F1.minus.bw
Orange_F1.plus.bw
Purple_X1.minus.bw
Purple_X1.plus.bw
Orange_X1.minus.bw
Orange_X1.plus.bw
[0 - 0.50]
[0 - 10.00]
Gene
MSTRG.9120=asDcMyb7
DCAR_010745=DcMyb7

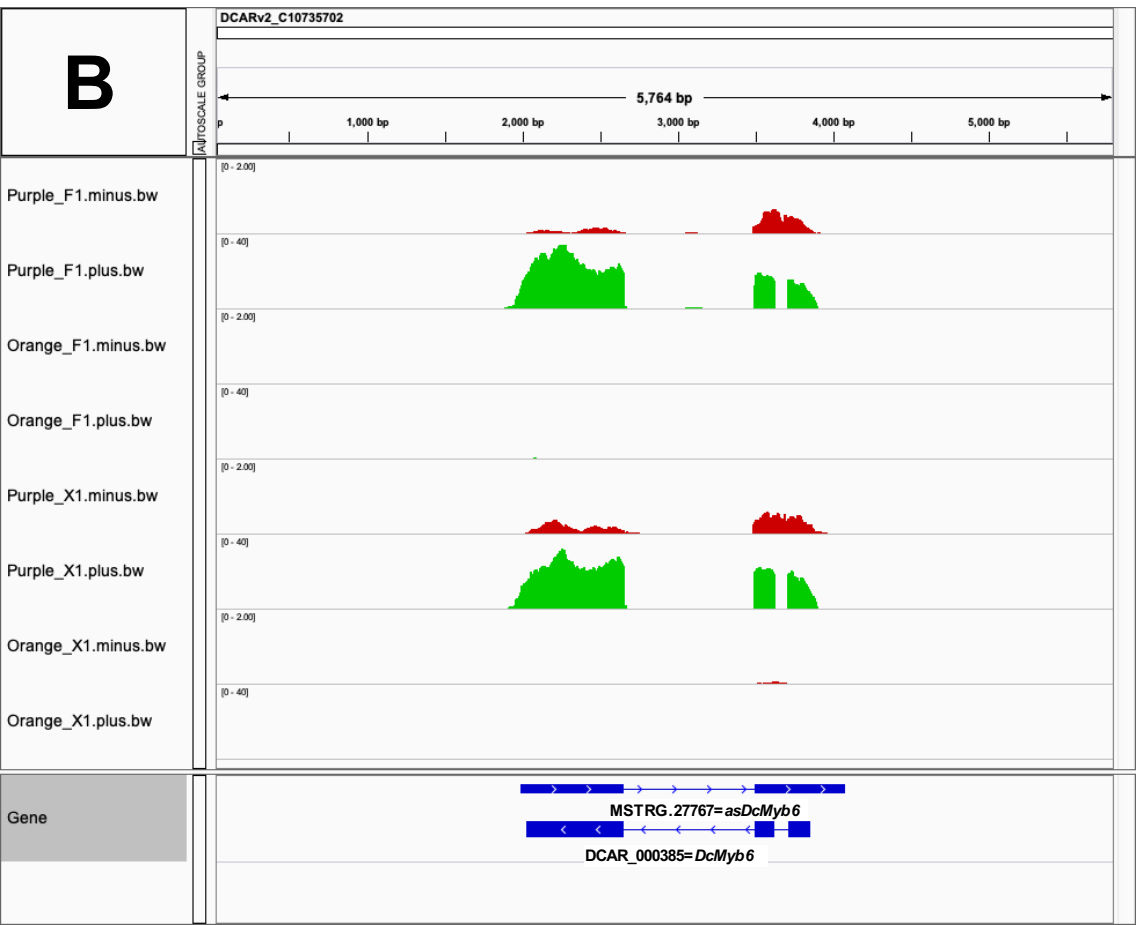
B
DCARv2_C10735702
AUTOSCALE GROUP
5,764 bp
1,000 bp
2,000 bp
3,000 bp
4,000 bp
5,000 bp
Purple_F1.minus.bw
Purple_F1.plus.bw
Orange_F1.minus.bw
Orange_F1.plus.bw
Purple_X1.minus.bw
Purple_X1.plus.bw
Orange_X1.minus.bw
Orange_X1.plus.bw
[0 - 2.00]
[0 - 40]
Gene
MSTRG.27767=asDcMyb6
DCAR_000385=DcMyb6